ACS Catalysis

Article

Kinetics and Mechanism of the Gold-Catalyzed Intermolecular Hydroalkoxylation of Allenes with Alcohols

Robert J. Harris, Robert G Carden, alethea duncan, and Ross A. Widenhoefer

ACS Catal., **Just Accepted Manuscript** • DOI: 10.1021/acscatal.8b02211 • Publication Date (Web): 10 Aug 2018

ACS Publications

is published by the American Chemical Society. 1155 Sixteenth Street N.W., Washington, DC 20036

Kinetics and Mechanism of the Gold-Catalyzed Intermolecular Hydroalkoxylation of Allenes with Alcohols

Robert J. Harris, Robert G. Carden, Alethea N. Duncan, and Ross A. Widenhoefer*

Duke University, Department of Chemistry, French Family Science Center, Durham, North Carolina, 27708

rwidenho@chem.duke.edu

Abstract: The mechanism of the hydroalkoxylation of 3-methyl-1,2-butadiene (**1**) with 1-phenylpropan-1-ol (**2**) catalyzed by (IPr)AuOTf in toluene has been evaluated through a combination of kinetic analysis, deuterium labeling studies, and *in situ* spectral analysis of catalytically active mixtures. These data are consistent with a mechanism involving endergonic conversion of (IPr)AuOTf and **1** to the cationic gold π-allene complex (IPr)Au[η^2-$H_2C{=}C{=}CMe_2$][OTf] (**5**•OTf), which undergoes outer-sphere addition of **2** followed by rapid protodemetallation to form 1-(3-methyl-2-butenyloxy)propyl)benzene (**3a**) as the kinetic product. The microscopic rate constants associated with the formation and consumption of **5**•OTf are of similar magnitude, such that the kinetic behavior of catalytic hydroalkoxylation changes as a function of the relative and absolute concentrations of allene and alcohol.

Keywords: hydrofunctionalization, C−O bond formation, mechanism, kinetics, gold, NHC, allene

Introduction

Cationic gold(I) complexes have emerged as a highly effective catalysts for the π-activation of C–C multiple bonds, most notably for the cycloisomerization of 1,*n*-enynes and for the hydrofunctionalization of C–C multiple bonds with H–X nucleophiles (X = C, N, O).[1-7] Within this latter family of transformations, allenes have attracted considerable attention as substrates for gold(I)-catalyzed hydrofunctionalization owing to the facility of the transformations,[4] the potential for stereospecific[5-7] and enantioselective transformations,[3] and the wide range of nucleophiles that undergo allene hydrofunctionalization including water, alcohols, carbamates, esters, carboxamides, ureas, thiols, and alkyl and aryl amines, electron-rich arenes, and activated methylene compounds.[4] Similarly, gold(I)-catalyzed allene hydrofunctionalization has been applied to the total synthesis of a number of natural products[2] including (–)-Rhazinilam,[8] flinderoles B and C,[9] swainsonine,[10] bejarol,[11] jaspine B,[12] indoxamycin,[13] and (–)-funebrine.[14]

Along with the development of the synthetic aspects of gold(I)-catalyzed allene hydrofunctionalization, there has been considerable interest in understanding the mechanisms of these processes,[15] although much of this effort has focused on computational analysis.[16,17] Experimental efforts in this area[18] have focused primarily on the synthesis and interrogation of potential intermediates in gold(I)-catalyzed allene hydrofunctionalization, including cationic gold(I) π-allene complexes,[19,20] neutral gold vinyl complexes,[6,18,21-24] and *gem*-diaurated vinyl complexes,[18,22,23] and on the stereochemical analysis of gold-catalyzed allene hydrofunctionalization.[25-27] These latter studies have established the net *anti*-addition of the H–X bond of the nucleophile across a C=C of the allene, consistent with mechanisms involving outer-sphere attack of the nucleophile on a gold π-allene complex.[25-27]

Much less experimental information is available regarding the behavior of these potential intermediates under catalytic conditions, including information regarding the catalyst resting state(s), turnover-limiting and regio- and/or stereochemical determining steps, and the nature of the reactive

gold allene intermediates. Furthermore, extant experimental information is restricted largely to intramolecular hydrofunctionalization processes. For example, Gagné showed that a cationic bis(gold) vinyl complex accumulated in solution during the gold(I)-catalyzed intramolecular hydroarylation of allenes, which implicated a mechanism involving turnover-limiting protodeauration.[22] A subsequent study by Widenhoefer and Gagné of the hydroalkoxylation of 2,2-diphenylhexa-4,5-dien-1-ol catalyzed by [P(*t*-Bu)$_2$*o*-biphenyl]AuOTs supported a mechanism involving reversible C–O bond formation followed by turnover-limiting protonolysis of a mono(gold) vinyl complex that occurred competitively with formation of an inactive bis(gold) vinyl complex.[23,28] In comparison, Lalic's investigation of the intramolecular hydroalkoxylation of γ-hydroxy allenes catalyzed by a gold carboxylate complex supported a mechanism involving irreversible C–O bond formation followed by turnover-limiting protodeauration of a mono(gold) vinyl complex without competing formation of bis(gold) vinyl complexes.[6]

In what represents the only kinetic and mechanistic analysis of gold(I)-catalyzed intermolecular allene hydrofunctionalization, Toste and Goddard have reported a combined kinetic/computational analysis of the hydroamination of 1,7-diphenylhepta-3,4-diene with methyl carbazate catalyzed by (PPh$_3$)AuNTf$_2$. Here, authors invoked a "two-step, no intermediate" mechanism involving turnover-limiting isomerization of a gold η^2-allene complex to a gold η^1-allylic cation transition state that is trapped by methyl carbazate either prior to or after progression to the achiral η^1-allylic cation.[7] Experimentally, this conclusion was supported by the ~zero-order dependence of the rate on methyl carbazate concentration coupled with assignment of the gold π-allene complex [(Ph$_3$P)Au(η^2-PhCH$_2$CH$_2$C=C=CCH$_2$CH$_2$Ph)]$^+$ (**A**) as the catalyst resting state on the basis of *in situ* ^{31}P NMR analysis and independent synthesis. However, Widenhoefer and Brooner subsequently demonstrated that the species assigned by Toste and Goddard as π-allene complex **A** is rather the catalyst decomposition product [(PPh$_3$)$_2$Au]$^+$,[20] and without clear delineation of the catalyst resting state(s), zero-order rate

dependence on nucleophile concentration need not be attributed to turnover-limiting allene isomerization.

Herein we report the mechanistic analysis of the gold(I)-catalyzed intermolecular hydroalkoxylation of 3-methyl-1,2-butadiene (**1**) with 1-phenylpropan-1-ol (**2**), which forms primary allylic ether **3a** with high regioselectivity relative to tertiary allylic ether **4a** (eq 1).[25] This study includes the kinetic and spectroscopic analysis of catalytic mixtures, deuterium-labeling studies, and independent synthesis of potential intermediates. We targeted gold-catalyzed hydroalkoxylation for this study owing to the high efficiency of these processes[25] and because aliphatic alcohols are representative of the weakly basic nucleophiles typically employed in gold(I)-catalyzed allene hydrofunctionalization.[4] The results of these studies are in accord with a mechanism involving reversible, endergonic formation of a cationic gold π-allene complex that undergoes irreversible, outer-sphere attack by alcohol on an η^2-allene complex followed by rapid protodeauration.

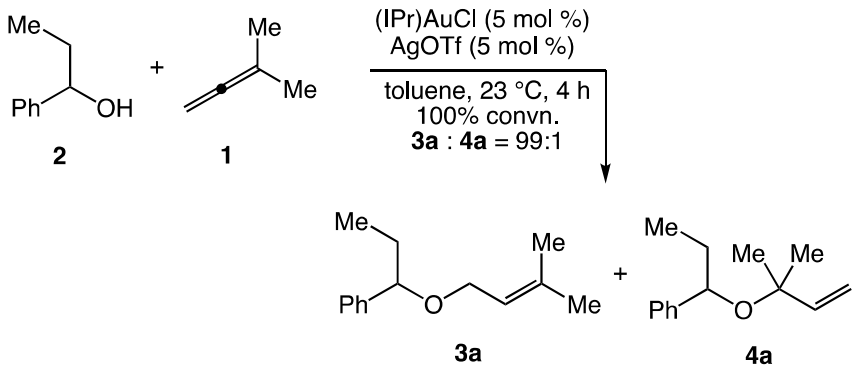

eq 1

RESULTS AND DISCUSSION

Kinetics of the Gold(I)-Catalyzed Hydroalkoxylation of excess 1 with 2. Toward an understanding of the mechanism of gold(I)-catalyzed intermolecular allene hydroalkoxylation, we investigated the kinetics of the reaction of **1** with **2** catalyzed by (IPr)AuOTf in toluene under conditions of excess allene **1**. In these studies, the single-component catalyst (IPr)AuOTf was employed in preference to a mixture of (IPr)AuCl and AgOTf to avoid potential complications associated with the

presence of silver salts either as co-catalysts or byproducts of catalyst activation.[29] In an initial experiment, a toluene solution of **1** (1.6 M), **2** (0.16 M), hexadecane (internal standard), and a catalytic amount of (IPr)AuOTf (15 mM) was stirred at 30 °C and analyzed periodically by GC. A plot of ln[**2**] versus time was linear to >3 half-lives with a pseudo-first-order rate constant of $9.8 \pm 0.4 \times 10^{-4}$ s^{-1} (Figure 1, Table 1, entry 1), which established first-order dependence of the rate on alcohol concentration under these conditions. Importantly, no significant (≤2%) formation of the regioisomeric allenyl alcohol **4a** was detected throughout complete conversion of **1** and **2** to **3a**.

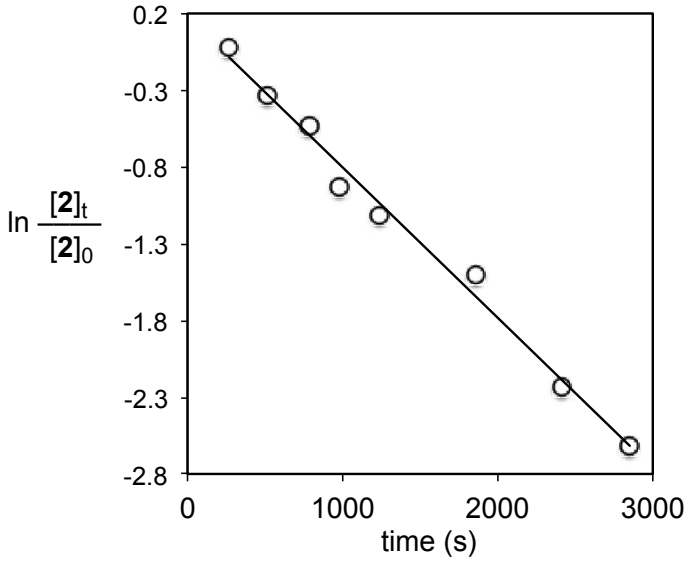

Figure 1. Pseudo-first-order plot for the hydroalkoxylation of **1** (1.6 M) with **2** (0.16 M) catalyzed by (IPr)AuOTf (16 mM) in toluene at 30 °C.

Table 1. Pseudo-first-order rate constants for the hydroalkoxylation of **1** with **2** catalyzed by (IPr)AuOTf in toluene at 30 °C.

entry	[**1**] (M)	[**2**] (M)	[cat] (mM)	additive (mM)	$(10^4)k_{obs}$ (s^{-1})
1	1.6	0.16	15	—	9.8 ± 0.4
2	0.78	0.16	15	—	5.4 ± 0.2
3	1.2	0.16	15	—	7.1 ± 0.4
4	2.3	0.16	15	—	11.9 ± 0.3
5	3.1	0.16	15	—	12.8 ± 0.5
6	1.6	0.16	8.2	—	5.4 ± 0.4
7	1.6	0.16	30	—	17.1 ± 0.6
8	1.6	0.16	16	Bu_4NOTf (16)	4.0 ± 0.2
9	1.6	0.16	16	Bu_4NOTf (24)	2.39 ± 0.08
10	1.6	0.16	15	Bu_4NOTf (77)	1.9 ± 0.2
11	1.6	0.16	15	HOTf (8.6)	4.4 ± 0.3
12	1.6	0.16	15	**3a** (75)	10.1 ± 0.4
13	1.6	0.16	15	—	11 ± 1
14[a]	0.18	0.90	18	—	3.39 ± 0.01
15	0.18	1.8	18	—	3.06 ± 0.02
16	0.18	2.7	18	—	2.71 ± 0.01
17	0.14	1.0	6.0	—	0.834 ± 0.007
18	0.14	1.0	13	—	2.49 ± 0.03
19	0.14	1.0	15	—	3.00 ± 0.07
20	0.14	1.0	20	—	4.06 ± 0.03
21	0.14	1.0	45	—	8.35 ± 0.15
22[a]	0.14	1.0	15	—	3.03 ± 0.02

[a]1-Phenylpropan-1-ol-*O*-*d* (**2**-*O*-*d,* ~90% *d*) was used in this reaction.

To determine the dependence of the rate of gold-catalyzed hydroalkoxylation on allene concentration, pseudo-first-order rate constants for the gold-catalyzed reaction of **1** with **2** (0.16 M) were determined as a function of allene concentration from 0.78 to 3.1 M (Table 1, entries 1-5). A plot of k_{obs} versus [**1**] revealed positive, non-linear dependence of the rate on allene concentration, consistent with a kinetic order between zero and one (Figure 2). To determine the dependence of the

rate of allene hydroalkoxylation on catalyst concentration, pseudo-first-order rate constants for the hydroalkoxylation of **1** (1.6 M) with **2** (0.16 M) were determined as a function of catalyst concentration from 8.2 to 30 mM (Table 1, entries 1, 6, and 7). A plot of k_{obs} versus [(IPr)AuOTf] was linear (Figure 3), which established the first-order dependence of the rate on catalyst concentration.

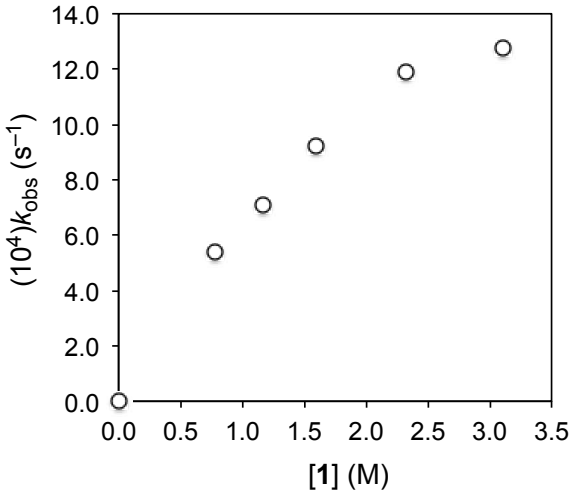

Figure 2. Allene concentration dependence of the rate of hydroalkoxylation of **1** (0.78 - 3.1 M) with **2** (0.16 M) catalyzed by (IPr)AuOTf (15 mM) in toluene at 30 °C.

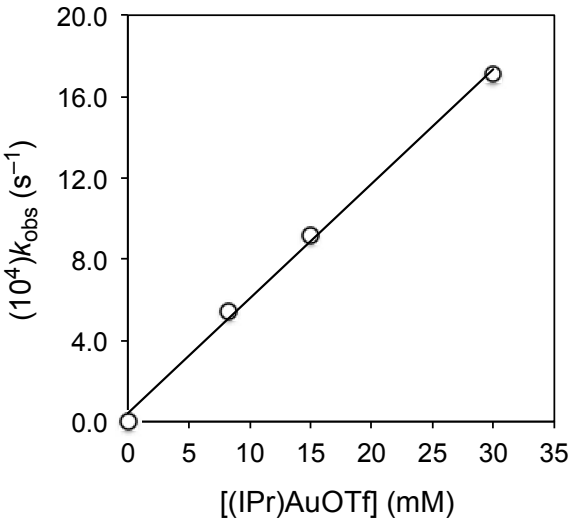

Figure 3. Plot of pseudo-first-order rate constants versus catalyst concentration for the hydroalkoxylation of **1** (1.6 M) with **2** (0.16 M) catalyzed by (IPr)AuOTf (0-30 mM) in toluene at 30 °C**.**

To determine the dependence of the rate of gold-catalyzed hydroalkoxylation on exogenous triflate ion concentration, pseudo-first-order rate constants for the reaction of **1** (1.6 M) with **2** (0.16 M) catalyzed by (IPr)AuOTf (16 mM) were determined as a function of tetrabutylammonium triflate concentration from 16 to 77 mM (Table 1, entries 8-10). The corresponding plot of pseudo-first-order rate constants versus the concentration of tetrabutylammonium triflate established inhibition of the rate of hydroalkoxylation by exogenous triflate (Figure 4). Similarly, gold-catalyzed reaction of **2** with excess **1** that contained triflic acid (8.6 mM) was ~50% slower than in the absence triflic acid (Table 1, entries 1 and 11). The rate of gold-catalyzed reaction of **2** with excess **1** that contained allylic ether **3a** (75 mM) in toluene was not significantly different from the rate of hydroalkoxylation in the absence of excess **3a** (Table 1, entries 1 and 12). Gold-catalyzed deuterioalkoxylation of **2** with 1-phenylpropan-1-ol-*O*-*d* (**2**-d_1; ~90% *d*) formed **3a**-d_1 with 77% deuterium incorporation exclusively at the internal vinylic position of **3a**-d_1 and with no significant deuterium kinetic isotope effect (KIE): k_H/k_D = 1.1 ± 0.1 (eq 2; Table 1, entries 1 and 13).

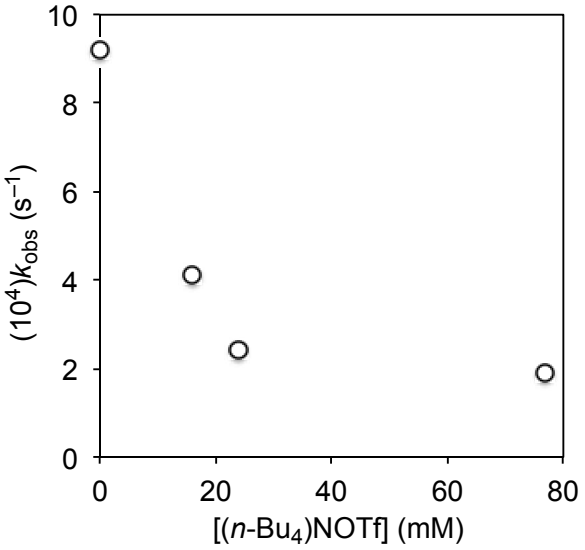

Figure 4. Plot of the concentration of tetrabutylammonium triflate versus k_{obs} for the reaction of **1** (1.6 M) with **2** (0.16 M) catalyzed by (IPr)AuOTf (~15 mM).

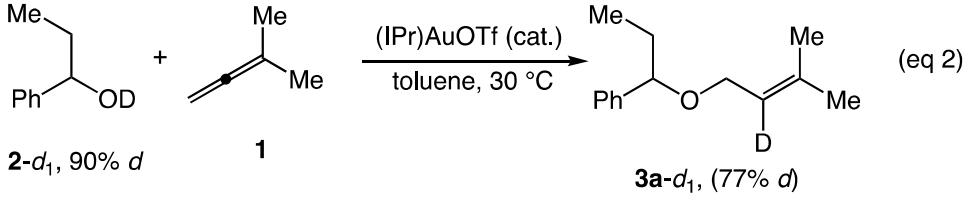

Kinetics of the Gold(I)-Catalyzed Hydroalkoxylation of 1 with excess 2. In a second set of experiments, we analyzed the kinetics of the gold-catalyzed hydroalkoxylation of allene **1** with alcohol **2** under conditions of excess alcohol. In one experiment, a solution of **1** (0.18 M), **2** (0.90 M), $CHCl_3$ (internal standard) and (IPr)AuOTf (18 mM) in toluene-d_8 at 30 °C was analyzed periodically by ^{1}H NMR spectroscopy. A plot of ln[**1**] versus time was linear to >3 half-lives with a pseudo-first-order rate constant of k_{obs} = 3.39 ± 0.01 × 10^{-4} s^{-1} (Figure 5, Table 1, entry 14), which established first-order dependence of the rate on allene concentration under these conditions. As was the case with hydroalkoxylation of **1** under conditions of excess allene, no significant (≤2%) formation of the regioisomeric allenyl alcohol **4a** was observed during the conversion of **1** and **2** to **3a**.

To determine the dependence of the rate of hydroalkoxylation on alcohol concentration, pseudo-first-order rate constants for the disappearance of **1** were determined as a function of [**2**] from 0.9 to 2.7 M (Table 1, entries 14-16). A plot of the corresponding pseudo-first-order rate constants versus $[\mathbf{2}]_0$ revealed that the rate of hydroalkoxylation displayed near zero-order dependence on alcohol concentration over this range (Figure 6), in sharp contrast to the first-order rate dependence on alcohol concentration under conditions of excess allene. To determine the dependence of the rate on catalyst concentration, pseudo-first-order rate constants for the hydroalkoxylation of **1** (0.15 M) with **2** (1.0 M) were determined as a function of catalyst concentration from 8.2 to 30 mM (Table 1, entries 12, 17-21). A plot of k_{obs} versus [(IPr)AuOTf] was linear (Figure 7), which established the first-order dependence of the rate of hydroalkoxylation on catalyst concentration and overall the second-order rate law under these conditions: rate = $k'[\mathbf{1}][(\text{IPr})\text{AuOTf}]$ where $k' = 1.88 \pm 0.01 \times 10^{-2}\ \text{M}^{-1}\ \text{s}^{-1}$ at $[\mathbf{2}]_0 = 0.9$ M. Gold-catalyzed deuterioalkoxylation of **1** with excess 1-phenylpropan-1-ol-*O*-*d* (**2**-d_1; 90% *d*) occurred with no detectable KIE ($k_H/k_D = 1.00 \pm 0.03$; Table 1, entries 19 and 22).

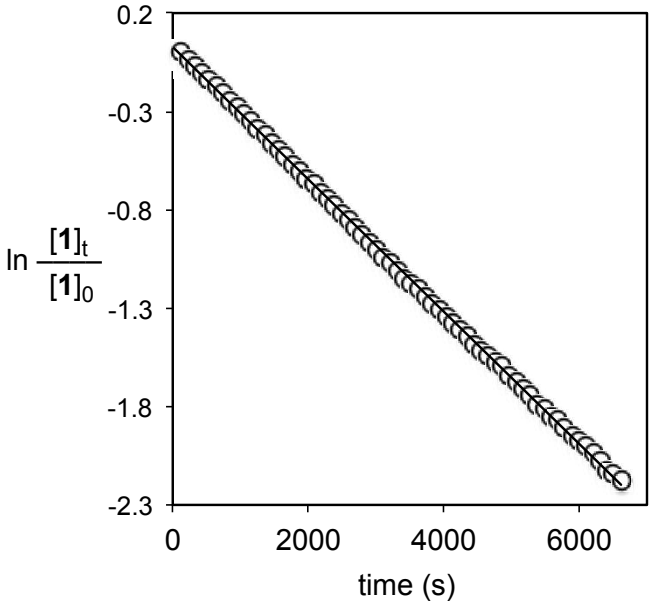

Figure 5. Pseudo-first-order plot for the hydroalkoxylation of **1** (0.18 M) with **2** (0.90 M) catalyzed by (IPr)AuOTf (18 mM) in toluene-d_8 at 30 °C.

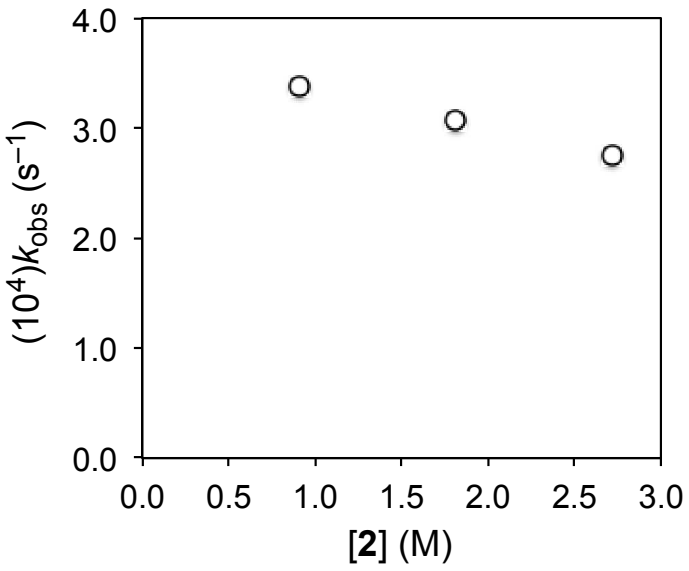

Figure 6. Plot of pseudo-first-order rate constants versus alcohol concentration for the hydroalkoxylation of **1** (0.18 M) with **2** (0.90 - 2.7 M) catalyzed by (IPr)AuOTf (18 mM) in toluene-d_8 at 30 °C.

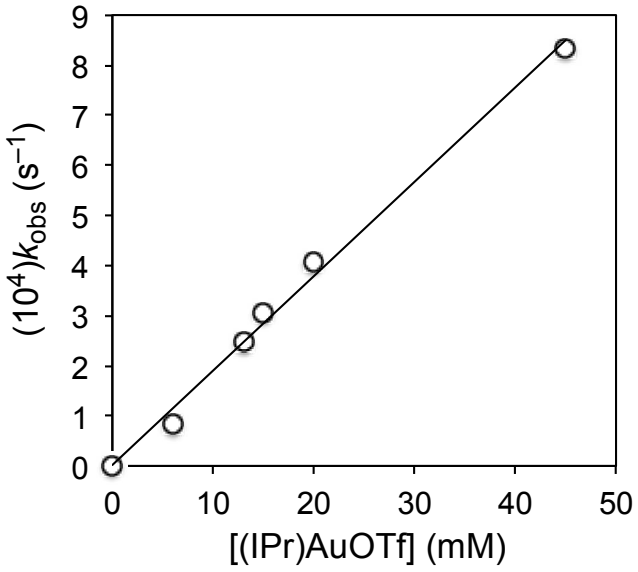

Figure 7. Plot of pseudo-first-order constants versus catalyst concentration for the hydroalkoxylation of **1** (0.15 M) with **2** (1.0 M) catalyzed by (IPr)AuOTf (0-45 mM) in toluene at 30 °C.

Spectroscopic Analysis of Catalytic Mixtures. A series of experiments were performed to gain insight into the resting state(s) of the gold-catalyzed hydroalkoxylation of **1** with **2**. Unfortunately, the absence of a phosphine supporting ligand precluded analysis of catalytically active mixtures by ^{31}P NMR spectroscopy and ^{1}H NMR spectroscopy alone proved unsuitable for this task due to excessive broadening and poor dispersion of chemical shifts. We therefore employed the ^{13}C-labeled gold complex (IPr*)AuOTf (IPr* = IPr-1-$^{13}C_1$) which exploits the diagnostic and generally well dispersed carbene C1 resonances of potential reaction intermediates. For example, the carbene C1 resonance of (IPr*)AuOTf appears at δ 163 in the ^{13}C NMR spectrum as compared to δ ~180 for cationic gold π-allene and alkene complexes,[19,30] and ~200 for neutral IPr gold σ-vinyl[31] and cationic IPr bis(gold) vinyl complexes.[32]

In one experiment, allene **1** was added incrementally (0.50, 1.0, 1.5, 2.0 M) to a solution of (IPr*)AuOTf (~30 mM) in toluene-d_8 and analyzed after each addition by ^{13}C NMR spectroscopy at 30 °C (eq 3). As the concentration of **1** increased, the carbene ^{13}C resonance of (IPr*)AuOTf broadened and shifted slightly downfield and when the concentration of **1** reached ~2 M, a broad resonance at δ ~180, assigned to gold π-allene complex (IPr*)Au(η^2-H_2C=C=CMe_2)]$^+$ OTf$^-$ (**5**-$^{13}C_1$), was observed along with the resonance of (IPr*)AuOTf at δ 165, although the excessive broadening of these resonances precluded accurate determination of the relative concentrations (eq 3, Figure 8). Nevertheless, these observations are consistent with the (1) endergonic conversion of (IPr*)AuOTf and **1** to **5** and (2) the formation of kinetically-relevant concentrations of **5** in the presence of excess **1**. The resulting solution of (IPr*)AuOTf (30 mM) and excess **1** (~2 M) was then treated with alcohol **2** (0.14 M) and monitored periodically by ^{13}C NMR spectroscopy at 30 °C. The broad resonances at δ 165 and 180 persisted throughout complete conversion of **1** and **2** to **3a** ($t_{1/2}$ = 20 min) without the appearance of any additional carbene resonances. These observations established the gold triflate complex (IPr)AuOTf and the gold π-allene complex **5** as the predominant gold complexes present under catalytic conditions.

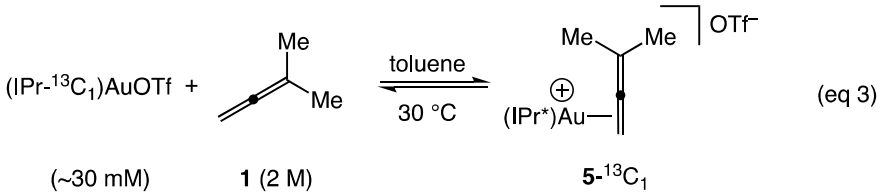

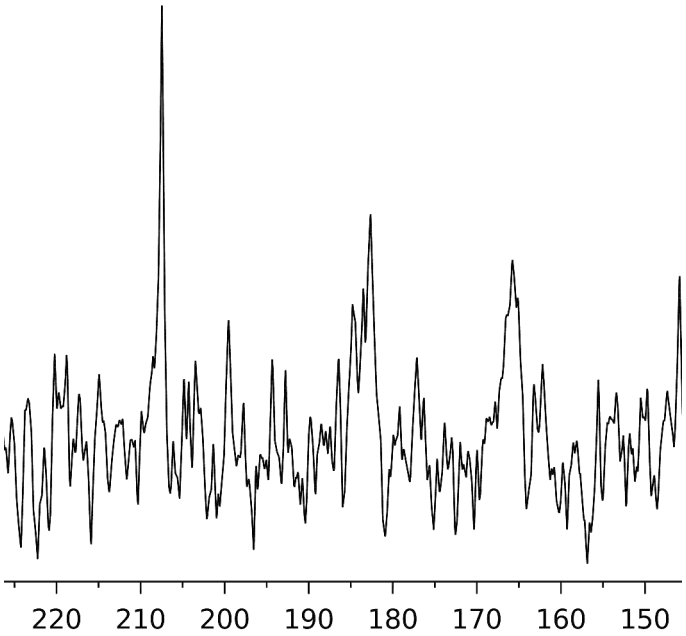

Figure 8. Portion of the ^{13}C NMR spectrum of a mixture of **1** (2.0 M) and (IPr*)AuOTf (~30 mM) in toluene-d_8 at 30 °C. The resonance at δ ~208 corresponds to the sp carbon atom of **1**.

In a second experiment, alcohol **2** was added incrementally to a toluene-d_8 solution of (IPr*)AuOTf (~30 mM) at 30 °C and analyzed after each addition by ^{13}C NMR spectroscopy. Addition of a large excess of **2** (~1.5 M) produced no detectable change in the ^{13}C NMR resonance corresponding to (IPr*)AuOTf (δ 163) nor were any other carbene resonances observed (eq 4). These observations indicate that the equilibrium constant for the conversion of (IPr*)AuOTf to gold alcohol complex [(IPr)Au(□□CH(Et)Ph)]$^+$ (**6**) is exceedingly small.[33,34] The resulting solution of (IPr*)AuOTf and excess **2** was then treated with allene **1** (0.14 M) and the solution was monitored periodically by ^{13}C NMR

spectroscopy at 30 °C. The sharp resonance of (IPr*)AuOTf at δ 163 broadened slightly upon addition of allene but otherwise remained unchanged throughout complete conversion of **1** and **2** to **3** without the appearance of any additional carbene resonances, which established (IPr*)AuOTf as the predominant gold-containing species present during catalysis under conditions of excess alcohol.

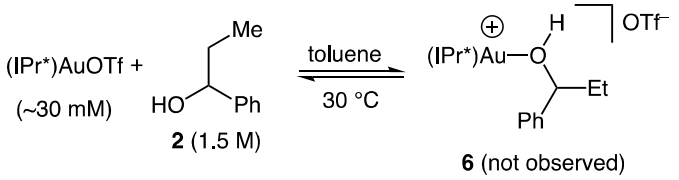

(eq 4)

Kinetic Regioselectivity of Hydroalkoxylation. Paton and Maseras have previously investigated the mechanism of the hydroalkoxylation of **1** with methanol catalyzed by (IPr)Au$^+$ employing DFT calculations.[17] This analysis supported a mechanism involving outer-sphere addition of methanol to the more substituted terminus of **1** to form tertiary allylic ether **4b** followed by secondary isomerization of **4b** to primary allylic alcohol **3b** via outer-sphere addition of methanol to the γ-carbon atom of the π-(allylic ether) complex **I** followed by elimination of methanol (Scheme 1).[17] The gold-catalyzed transposition of allylic ethers in the presence of alcohol has been validated experimentally by us and others.[35] Furthermore, Lee has shown that gold(I)-catalyzed hydroalkoxylation of allene **1** with excess primary alcohol in DMF at 0 °C leads to selective formation of the corresponding tertiary allylic ether (eq 5).[36]

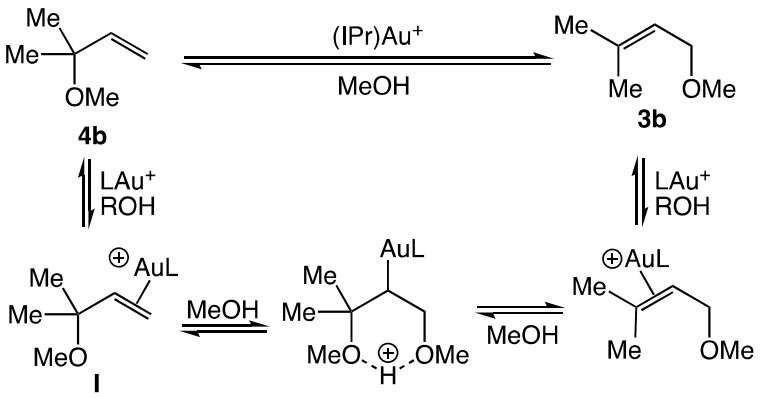

Scheme 1. Proposed mechanism for the gold-catalyzed isomerization of tertiary allylic ether **4b** to primary allylic alcohol **3b** in the presence of methanol.

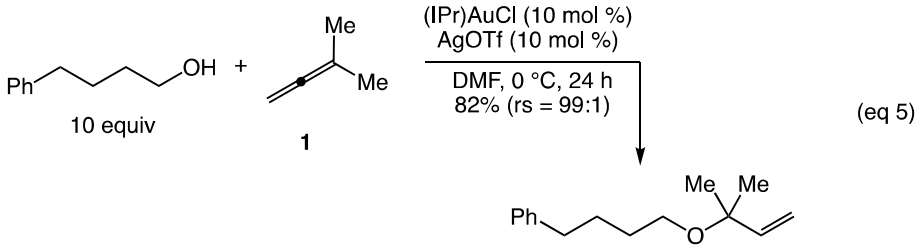

For the reasons outline in the preceding paragraph, we sought to evaluate the possibility that **3a** was formed via secondary isomerization of **4a** in the gold-catalyzed hydroalkoxylation of **1** with **2**. As noted above, periodic analysis of the gold(I)-catalyzed conversion of **1** and **2** to **3a** under conditions of either excess allene or alcohol revealed no detectable accumulation of tertiary allylic alcohol **4a**. Therefore, if **4a** were an intermediate in the gold(I)-catalyzed conversion of **1** and **2** to **3a**, conversion of **4a** to **3a** under reaction conditions would have to be much faster than the formation of **3a**. Importantly, a pair of experiments employing methanol as nucleophile argue strongly against this possibility and, rather point to formation of **3a** as the kinetic product of hydroalkoxylation. Specifically, reaction of **1** (0.8 M) with methanol (0.8 M) and a catalytic amount of (IPr)AuOTf (~30 mM) at 23 °C reached >95% conversion after 2 h to form **3b** as the exclusive product (Scheme 2). In comparison, treatment of a 1:1 mixture of **4b** (0.8 M) and methanol (~0.8 M) with a catalytic amount of (IPr)AuOTf (~30 mM) at 23 °C

for 2 h led to no detectable consumption of **4b** or formation of **3b** as determined by ^{1}H NMR analysis of the crude reaction mixture.

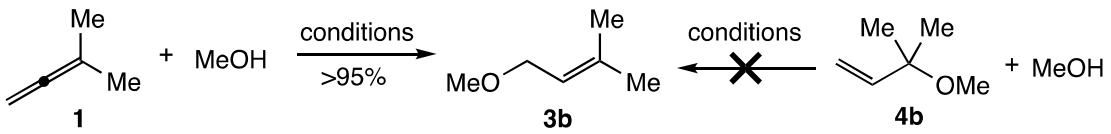

conditions = (IPr)AuCl (5 mol %), AgOTf (5 mol %), toluene, 23 °C, 2 h

Scheme 2. Gold-catalyzed reactions of **1** and **4b** with methanol.

Kinetic Model for the Hydroalkoxylation of 1 with 2. Although our analysis of the gold(I)-catalyzed reaction of **1** with **2** provides no direct insight into the stereochemistry of C–O bond formation, we have previously established the net anti-addition of the O–H bond of an alcohol across the C=C bond of an allene for both intra- and intermolecular gold-catalyzed hydroalkoxylation, and these observations are consistent with outer-sphere mechanisms for C–O bond formation.[25-27,37] We therefore interpreted the kinetics of the hydroalkoxylation of **1** with **2** catalyzed by (IPr)AuOTf in the context of the mechanism depicted in Scheme 3 involving reversible reaction of (IPr)AuOTf with **1** to form gold π-allene complex **5**•OTf,[19] outer-sphere addition of alcohol **2** to **5**•OTf to form the *O*-protonated gold σ-vinyl intermediate **II**, and rapid protodeauration to form gold π-allylic ether complex **III**•OTf that collapses to release **3** and close the catalytic cycle. Key assumptions made in the derivation of rate laws were that (1) protodeauration (**II** → **III**•OTf), and hence hydroalkoxylation, is irreversible, (2) gold triflate complex (IPr)AuOTf and gold π-allene complex **5**•OTf are the only complexes that accumulate under catalytic conditions ($[Au]_{tot}$ = [(IPr)AuOTf] + [**5**•OTf]), and (3) cationic π-complex **5** exists as the tight ion pair **5**•OTf in the non-polar reaction medium ($K_A[OTf^-] >> 1$; see below).

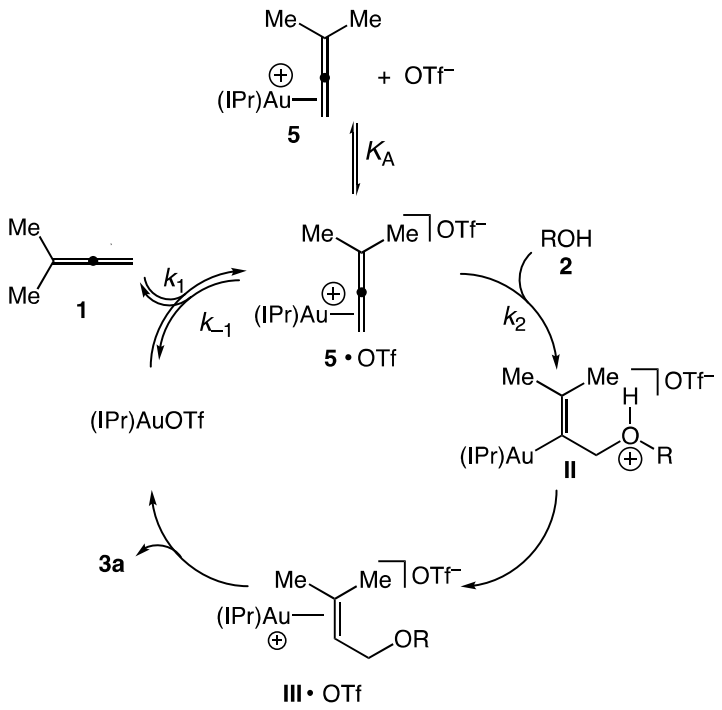

Scheme 3. Proposed mechanism for the gold-catalyzed hydroalkoxylation of **1** with **2.**

Within the mechanism depicted in Scheme 3, kinetic scenarios involving turnover-limiting protodeauration or deprotonation of **II** can be safely discounted on the basis of our experimental observations. For example, mechanisms involving reversible C–O bond formation followed by turnover-limiting protodeauration or deprotonation would be expected to display significant deuterium KIEs for deuterioalkoxylation and first-order dependence on [**2**] under all conditions, neither of which was observed experimentally. Importantly, both we[23] and Lalic[6] have observed large KIEs ($k_H/k_D > 5$) for gold-catalyzed intramolecular hydroalkoxylation/deuterioalkoxylation of allenes under conditions of turnover-limiting protodeauration. Similarly, mechanisms involving irreversible C–O bond formation followed by turnover-limiting protodeauration would be expected to display a significant KIE for deuterioalkoxylation, zero-order rate dependence on both [**1**] and [**2**] under all conditions, and the accumulation of mono(gold) or bis(gold) vinyl complexes under catalytic conditions, none of which were observed experimentally.

The observed change in the kinetic order of the gold-catalyzed hydroalkoxylation of **1** with **2** as a function of the **1**:**2** ratio points to a change in the resting state catalyst composition and/or the turnover-limiting step of catalysis, the latter of which requires that two or more microscopic steps within the catalytic cycle occur at similar rates. As such, application of the pre-equilibrium assumption to the reversible formation of gold π-allene complex **5**•OTf, which is often assumed valid for gold-catalyzed hydrofunctionalization processes, appears overly restrictive. Rather, application of the Bodenstein (steady state) approximation to gold π-allene complex **5**•OTf with no additional restrictions generates the rate law depicted in equation 6, which is of the same form as the Briggs-Haldane equation for enzyme kinetics.[38]

$$\text{rate} = \frac{k_1 k_2[\mathbf{1}][\mathbf{2}][\text{Au}]_{\text{tot}}}{k_{-1} + k_1[\mathbf{1}] + k_2[\mathbf{2}]} \qquad \text{(eq 6)}$$

$$\text{rate} = \frac{k_1 k_2[\mathbf{1}][\mathbf{2}][\text{Au}]_{\text{tot}}}{k_{-1} + k_1[\mathbf{1}]} \text{ when } k_2[\mathbf{2}] << k_{-1} + k_1[\mathbf{1}] \qquad \text{(eq 7)}$$

$$\text{rate} = k_1[\mathbf{1}][\text{Au}]_{\text{tot}} \text{ when } k_2[\mathbf{2}] >> k_{-1} + k_1[\mathbf{1}] \qquad \text{(eq 8)}$$

From the general rate equation for hydroalkoxylation of **1** with **2** (eq 6), we considered two limiting kinetic scenarios based on the relationship between the rate of C–O bond formation (k_2[**2**]) and the rates of interconversion of (IPr)AuOTf and **5**•OTf (k_1[**1**] and k_{-1}). In the case where C–O bond formation is much slower than is the interconversion of (IPr)AuOTf and **5**•OTf (k_2[**2**] << k_1[**1**] + k_{-1}), the rate equation simplifies to the two-term rate equation depicted in eq 7, which is of the same form as the Michaelis–Menten equation and which predicts first-order rate dependence on [**2**] and $[\text{Au}]_{\text{tot}}$, and between zero- and first-order dependence on [**1**]. This rate equation is of the same form as the experimental rate law determined for the gold-catalyzed reaction of **1** and **2** under conditions of excess allene **1**, which displayed first-order dependence on [**2**] and a positive, non-integer dependence on **1**.

In the case where C–O bond formation is much faster than is the interconversion (IPr)AuOTf and **5**•OTf (k_2[**2**] >> k_1[**1**] + k_{-1}), the rate equation depicted in eq 6 simplifies to the second-order rate equation depicted in eq 8 predicting first-order dependence of the rate on [**1**] and $[Au]_{tot}$ and zero-order dependence on [**2**]. This rate equation is of the same form as the experimental rate law determined for the gold-catalyzed reaction of **1** and **2** under conditions of excess alcohol **2** where rate = k'[**1**][(IPr)AuOTf], where the macroscopic rate constant k' corresponds directly to the microscopic rate constant k_1.

Rate equation 7, which describes the rate behavior of catalytic hydroalkoxylation under conditions of excess allene, can alternatively be represented at eq 9. Taking the reciprocal of the equation describing k_{obs} gives equation 10, which predicts a linear relationship between $1/k_{obs}$ and 1/[**1**] under conditions of excess allene at constant catalyst concentration with slope = $k_{-1}/k_1k_2[Au]_{tot}$ and with intercept = $1/k_2[Au]_{tot}$. Indeed a plot of the reciprocal of the experimentally-determined pseudo-first-order rate constants for the hydroalkoxylation of **1** under conditions of excess allene at constant catalyst concentration ([cat] = 16 mM) versus 1/[**1**] was linear with a slope = 1.15 ± 0.05 × 10^3 M s and intercept = 3.9 ± 0.4 × 10^2 s (Figure 9), from which values for the microscopic rate constant k_2 = 0.17 ± 0.02 s^{-1} M^{-1} and equilibrium constant k_1/k_{-1} = K_1 = 0.34 ± 0.02 M^{-1} were derived. Furthermore, using the value for k_1, which corresponds to the second-order rate constant for hydroalkoxylation under conditions of excess alcohol (k' = k_1 = 1.88 ± 0.01 × 10^{-2} s^{-1} M^{-1}), we likewise derived the value for rate constant k_{-1} = 5.6 ± 0.5 × 10^{-2} s^{-1}.

$$\text{rate} = k_{obs}[\mathbf{2}] \qquad \text{where } k_{obs} = \frac{k_1k_2[\mathbf{1}][Au]_{tot}}{k_{-1} + k_1[\mathbf{1}]} \qquad \text{(eq 9)}$$

$$\frac{1}{k_{obs}} = \frac{k_{-1}}{k_1k_2[\mathbf{1}][Au]_{tot}} + \frac{1}{k_2[Au]_{tot}} \qquad \text{(eq 10)}$$

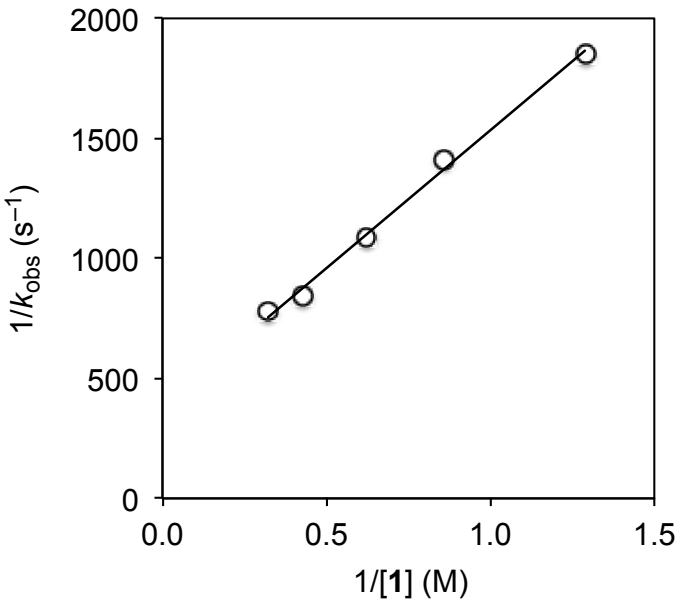

Figure 9. Plot of $1/k_{obs}$ versus 1/[**1**] for the hydroalkoxylation of **1** with **2** catalyzed by (IPr)AuOTf (15 mM) in toluene at 30 °C.

The equilibrium constant K_1 = 0.34 M^{-1} determined from the above analysis predicts an equilibrium ratio of (IPr)AuOTf:**5**•OTf ≈ 1.5:1 at [**1**] = 2 M and $[Au]_{tot}$ = 30 mM according to the relationship K_1 = [**5**•OTf]/[(IPr)AuOTf][**1**]. This value is consistent with our experimental observations regarding the formation of **5**•OTf from (IPr)AuOTf and **1**, considering the low sensitivity of our ^{13}C NMR measurements. Less clear is that the values determined for the microscopic rate constants k_1, k_{-1}, and k_2 validate the limiting conditions k_2[**2**] << k_{-1} + k_1[**1**] (eq 7) and k_2[**2**] >> k_{-1} + k_1[**1**] (eq 8) corresponding to the experimental conditions of excess allene and excess alcohol, respectively. For example, the calculated values for k_1[**1**], k_{-1}, and k_2[**2**] under typical conditions of excess allene ([**1**] = 1.6 M, [**2**] = 0.16 M) are 0.034, 0.056, and 0.027 s^{-1}, respectively, and the calculated values for k_1[**1**], k_{-1}, and k_2[**2**] under general conditions of excess alcohol ([**1**] = 0.18 M, [**2**] = 1.8 M) are 0.0034, 0.056, and 0.31 s^{-1}, respectfully. However, here it should be noted that the value for k_1 employed in this analysis was determined under conditions of excess alcohol, whereas the values for k_2 and K_1 were determined under conditions of excess allene, under the assumption that the magnitudes of these microscopic rate

constants are invariant of the reaction conditions. One observation that suggests this may not be the case is the observed decrease in k_{obs}, where $k_{obs}/[Au]_{tot} = k_1$, with increasing [**2**] under conditions of excess alcohol (Figure 5), which suggests that k_1 may be larger under conditions of excess allene, although the origin of this rate/medium effect remains unclear.

Ion Pairing and Role of Exogenous Triflate. The formation of ion pairs between non-coordinating anions and cationic transition metal complexes,[39] including cationic gold π-complexes,[40] is well established, with association constants that typically exceed 1×10^4 in CH_2Cl_2.[41,42] Furthermore, because log K_A for ion pair association typically scales with the reciprocal of the dielectric constant of the medium (*i.e.* 1/ε),[43] ion pairing of **5** with OTf^- is anticipated to be exceptionally strong in the non-polar reaction medium employed in catalytic hydroalkoxylation [$\varepsilon(CH_2Cl_2) = 8.93$; ε(toluene) = 2.38].[44-46] Importantly, ligand substitution of cationic transition metal complexes with strongly associated anionic ligands occurs through an interchange mechanism and displays zero-order rate dependence on the concentration of the anionic ligand.[39,41,42,47] In the context of gold(I)-catalyzed allene hydroalkoxylation, the presence of strong ion pairing between **5** and OTf is consistent with the absence of any significant curvature of the plot of k_{obs} versus [(IPr)AuOTf] at constant, excess [**1**] (Figure 3). For example, under conditions of negligible ion pairing between **5** and OTf ($K_A[OTf^-] << 1$), equation 7 is replaced by eq 11 containing the term $k_{-1}K_A$[OTf] in the denominator.[48] Because $[OTf^-]$ would increase with increasing $[Au]_{tot}$ under conditions of negligible ion pairing, the rate dependence on catalyst concentration under such conditions would approach half-order, which was not observed (Figure 3).[49]

$$\text{rate} = \frac{k_1 k_2[\mathbf{1}][\mathbf{2}][\text{Au}]_t}{k_{-1}K_A[\text{OTf}^-] + k_1[\mathbf{1}]} \qquad \text{(eq 11)}$$

Under conditions of strong ion pairing between **5** and OTf^-, the observed inhibition of the rate of hydroalkoxylation by tetrabutylammonium triflate (Figure 4) points to the presence of an additional triflate-dependent pathway for the reversion of **5**•OTf to (IPr)AuOTf. Here, two points are worth noting.

Firstly, simply relaxing the condition of strong ion pairing between **5** and OTf (K_A[OTf] >> 1) does not account for the observed rate dependence on both catalyst and tetrabutylammonium triflate concentration. In particular, in the case of a modest association constant for ion pairing between **5** and OTf^-, the rate dependence on triflate concentration would be most pronounced at the lowest triflate concentrations, such as in the determination of the rate dependence on (IPr)AuOTf concentration. However, as was noted above, no significant deviation from linearity was observed for a plot of k_{obs} versus [(IPr)AuOTf] from 0 - 30 mM (Figure 3). Secondly, owing to the strong ion pairing between tetrabutylammonium and triflate in the non-polar reaction medium[50] and the higher concentrations of triflate employed in these experiments relative to catalytic conditions (16 - 77 mM versus ≤30 mM, respectively), it is unlikely that this triflate-dependent pathway is relevant under conditions of catalytic hydroalkoxylation.

Because both **5**•OTf and tetrabutylammonium triflate are both strongly ion paired in the non-polar reaction medium,[50] a mechanism for the triflate-dependent reversion of **5**•OTf to (IPr)AuOTf involving direct attack of free triflate at the gold center of **5**•OTf followed by expulsion of allene **1** appears unlikely. Rather, allene for triflate ligand exchange presumably occurs via association of the [*n*-Bu_4N][OTf] ion pair with **5**•OTf to form an ion aggregate such as {[**5**][OTf]$_2$[(*n*-Bu_4N]} followed by ligand interchange.[51] This mechanism is analogous to that proposed by Romeo to rationalize the kinetics of the displacement of dimethyl sulfoxide from [Pt(Me_4En)(Me_2SO)Cl]Cl (Me_4En = (*N*,*N*,*N′*,*N′*-tetramethyldiaminoethane) by halide ions in CH_2Cl_2.[42]

Control of Regioselectivity in the Hydroalkoxylation of 1. The selective formation of the linear allylic ether **3a** in the gold-catalyzed hydroalkoxylation of **1** with **2** is intriguing owing both to the selective formation of tertiary allylic ether in the gold-catalyzed hydroalkoxylation of **1** in DMF (eq 5) and also the formation of the tertiary allylic carbamate in the closely related gold(I)-catalyzed hydroamination of **1** with benzyl carbamate (eq 12).[36,52] Our experimental data argue strongly against isomerization of **4a** to **3a** under reaction conditions and we can also safely rule out regiochemically-

determining formation of gold π-allene complex **5**•OTf owing to the facile ($\Delta G^{\ddagger} \leq 11$ kcal/mol) unimolecular interconversion of gold π-allene complexes **5** and **5'** via η^1-allene intermediate **IV** (Scheme 4).[19] The simplest rationale for the observed regioselectivity of the gold-catalyzed hydroalkoxylation of **1** with **2** is to invoke selective, irreversible attack of **2** at the less substituted allene terminus of **5**. However, we cannot rule out a mechanism involving rapid and reversible attack of **2** on **5'** that is superimposed on slower, irreversible attack of **2** on **5** and indeed, this mechanism might better account all the observations made in the context of gold-catalyzed allene hydrofunctionalization.[4.36.52] Supporting the feasibility of such a mechanism, gold vinyl complex **II'** generated via attack of **2** on **5'** is expected to be less stable than **II** owing to the diminished olefinic substitution and likewise, experimental and computational analysis of protodeauration supports the more facile protodeauration of **II** relative to **II'** owing to the presence of the electron-releasing olefinic methyl groups of **II**.[53]

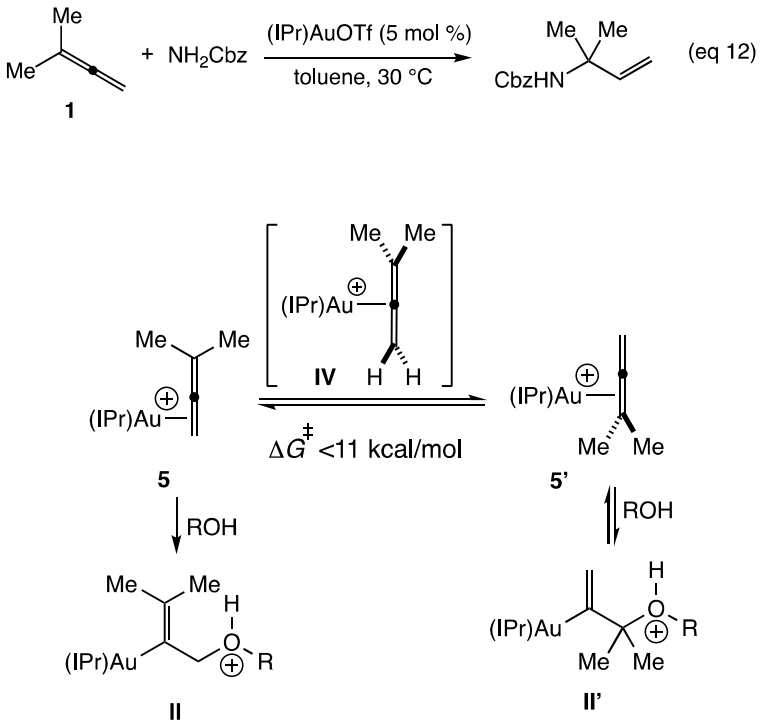

Scheme 4. Interconversion of gold π-allene complexes **5** and **5'** via η^1-allene intermediate **IV** and potential mechanism for regiocontrol in catalytic hydroalkoxylation.

Role of activated η^1-allene species in hydroalkoxylation. There has been considerable speculation regarding the potential attack of nucleophile on an activated η^1-allene species in gold-catalyzed allene functionalization processes,[16] most notably from the work of Toste and Goddard who invoked barrierless attack of methyl carbazate on the transition state leading to the η^1-allylic cation in the gold-catalyzed hydroamination of 1,7-diphenylhepta-3,4-diene.[7] Our analysis of the fluxional behavior of gold π-complexes containing aliphatic 1,1- and 1,3-disubstituted allenes established two distinct gold η^1-allene species: a lower energy ($\Delta G^{\ddagger}$ ≤11 kcal/mol) staggered η^1-allene intermediate or transition state (*e.g.* **IV**, Schemes 4 and 5) that leads to π-face exchange without allene stereomutation and a higher energy ($\Delta G^{\ddagger}$ ≥17.5 kcal/mol) planar η^1-allylic cation intermediate (*e.g.* **V**, Scheme 5) that leads that leads to both π-face exchange and allene stereomutation.[19,54,55]

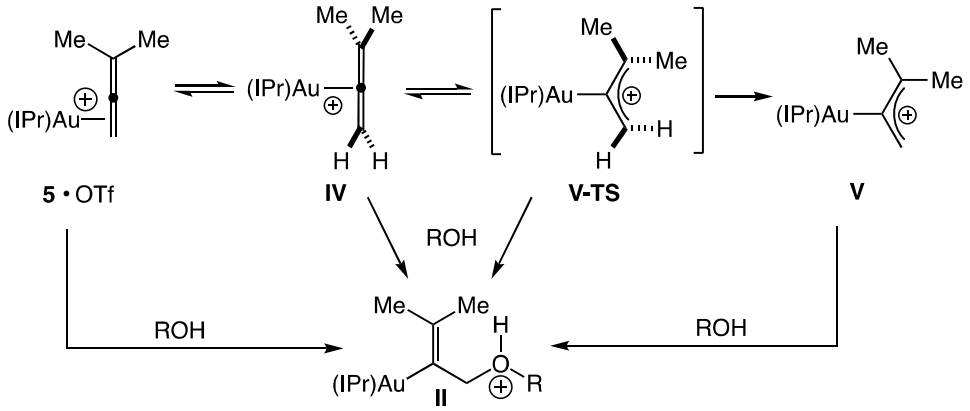

Scheme 5. η^2-Allene complex **5** and potential η^1-allene isomers.

In the context of the gold(I)-catalyzed hydroalkoxylation of **1** with **2**, a mechanism involving attack on the staggered η^1-allene intermediate **IV** is fully consistent with our kinetic data and is reminiscent of the slippage that is proposed to occur along the reaction coordinate for nucleophilic addition to a transition metal π-complex.[56] However, it appears unlikely that formation of **IV** ($\Delta G^{\ddagger}$ ≤11

kcal/mol) could become kinetically-controlling under any conditions. A mechanism involving outer-sphere attack of **2** on η^1-allylic cation **V** is likewise consistent with our kinetic data, and given the higher energy barrier for η^1-allylic cation formation, it is plausible that isomerization of **5** to **V** could become turnover-limiting under conditions of excess alcohol, as was observed experimentally. However, a mechanism involving outer-sphere attack of **2** on η^1-allylic cation **V**, generated either reversibly or irreversibly, provides no pathway for chirality transfer, which is common for the gold(I)-catalyzed hydroalkoxylation of axially chiral allenes.[5-7] Finally, a mechanism akin to that invoked by Toste and Goddard involving turnover-limiting generation and trapping of an η^1-allylic cation transition state (**V-TS**) is inconsistent with the observed first-order rate dependence on alcohol concentration under conditions of excess allene. Furthermore, such a pathway can be firmly discounted for the closely related gold-catalyzed intramolecular hydroalkoxylation of 2,2-diphenylhexa-4,5-dien-1-ol, where the energy barrier for C–O bond formation ($\Delta G^{\ddagger} \leq 13$ kcal/mol) occurred well below the threshold for allylic cation formation ($\Delta G^{\ddagger} \geq 17.5$ kcal/mol).[23]

Conclusions

In summary, we have investigated the kinetics and mechanism of the intramolecular hydroalkoxylation of 3-methyl-1,2-butadiene (**1**) with 1-phenylpropan-1-ol (**2**) catalyzed by (IPr)AuOTf in toluene. All of our data are consistent with the mechanism depicted in Scheme 3 involving endergonic formation of the cationic gold π-allene complex **5**, which exists as the tight ion pair **5**•OTf in the non-polar reaction medium. Outer-sphere addition of **2** to **5**•OTf followed by rapid protodemetallation and collapse of the resulting gold π-alkene complex **6** releases the primary allylic ether **3a** as the kinetic product and regenerates (IPr)AuOTf. The microscopic rate constants for the conversion of (IPr)AuOTf and **1** to **5**•OTf (k_1[**1**]), the collapse of **5**•OTf to (IPr)AuOTf and **1** (k_{-1}), and the rate of attack of **2** on **5**•OTf (k_2[**2**]) are similar enough such that (1) application of the pre-equilibrium assumption to the formation of **5**•OTf is not valid and (2) the rate behavior of catalytic hydroalkoxylation changes as a

function of the relative and absolute concentrations of **1** and **2**. Under conditions of excess allene **1**, the reaction rate displayed first-order dependence on [(IPr)AuOTf] and [**2**] and between zero- and first-order dependence on [**1**], while under conditions of excess alcohol **2**, the reaction rate displayed first-order dependence on [(IPr)AuOTf] and [**1**] and zero-order dependence on [**2**].

There has been a considerable speculation and debate concerning the role of counterion in gold(I)-catalyzed hydrofunctionalization reactions, in particular that outer-sphere C–X (X = N, O) bond formation is assisted by hydrogen bonding between the incoming nucleophile and the counterion.[57] Indeed, we have obtained evidence for counterion-assisted C–O bond formation in our investigation of gold-catalyzed intramolecular allene hydroalkoxylation.[58] The present investigation of the mechanism of the gold(I)-catalyzed hydroalkoxylation of **1** with **2** provides little additional insight in this regard. However, our data do show that potential triflate/alcohol hydrogen bonding cannot lead to significant O–H bond cleavage in the transition state for C–O bond formation, which would have been revealed by the presence of a KIE for the deuterioalkoxylation of **1** with **2**-*O*-*d*, which was not observed.

In comparison to counterion effects, there has been much less discussion regarding the effect of reaction medium on the kinetic behavior and mechanism of gold(I)-catalyzed hydrofunctionalization, and the present investigation points to the potential importance of such medium effects. In particular, the kinetics of catalytic hydroalkoxylation of **1** in toluene are dominated by the slow and endergonic conversion of (IPr)AuOTf to gold π-allene complex **5**•OTf, which was corroborated by *in situ* ^{13}C NMR analysis of the reaction of **1** with (IPr*)AuOTf. This behavior stands in sharp contrast to the reaction of **1** with (IPr)AuOTf in CD_2Cl_2, which forms **5** quantitatively with <2 equiv of allene.[19] Therefore, it is quite reasonable to assume that very different kinetic behavior of the gold-catalyzed hydroalkoxylation of **1** with **2** would be observed in more polar solvents, although predictions beyond this point are unwarranted owing to the absence of information regarding medium effects on the rate of C–O bond formation and/or on the equilibrium constants for the potentially competing formation of gold-nucleophile complexes.

■ ASSOCIATED CONTENT

■ AUTHOR INFORMATION

Corresponding Author

*E-mail: rwidenho@chem.duke.edu.

ORCID

Ross A. Widenhoefer: 0000-0002-5349-8477

Notes

The authors declare no competing financial interest.

Supporting Information

The Supporting Information is available free of charge on the ACS Publications website at DOI:xxxxxxx

Experimental procedures and derivation of differential rate equations (PDF)

■ ACKNOWLEDGMENTS We acknowledge the NSF (CHE-1465209) for support of this research. RGC was supported through a GAANN fellowship (P200A150114).

References

(1) a) Li, Y.; Li, W.; Zhang, J. Gold-Catalyzed Enantioselective Annulations. *Chem. Eur. J.* **2017**, *23*, 467 – 512; b) Quintavalla, A.; Bandini, M. Gold-Catalyzed Allylation Reactions. *ChemCatChem* **2016**, *8*, 1437-1453; c) Miróand, J.; del Pozo, C. Fluorine and Gold: A Fruitful Partnership. *Chem. Rev*. **2016**, *116*, 11924−11966; d) Hopkinson, M. N.; Tlahuext-Aca, A.; Glorius, F. Merging Visible Light Photoredox and Gold Catalysis. *Acc. Chem. Res*. **2016**, *49*, 2261−2272; e) Paioti, P. H. S.; Aponick, A. Gold-Catalyzed Transformation of Unsaturated Alcohols. *Top. Curr. Chem*. **2015**, *357*, 63–94; f) Dorel, R.; Echavarren, A. M. Gold(I)-Catalyzed Activation of Alkynes for the Construction of Molecular Complexity. *Chem. Rev*. **2015**, *115*, 9028−9072; g) Asiria, A. M.; Hashmi, A. S. K. Gold-Catalysed

Reactions of Diynes. *Chem. Soc. Rev*. **2016**, *45*, 4471-4503; h) Liu, L.; Zhang, J. Gold-Catalyzed Transformations of α-Diazocarbonyl Compounds: Selectivity and Diversity. *Chem. Soc. Rev.* **2016**, *45*, 506-516; i) Shin, S. Gold-Catalyzed Carbene Transfer Reactions. *Top. Curr. Chem*. **2015**, *357*, 25–62; j) Michelet, V. Gold-Catalyzed Domino Reactions. *Top. Curr. Chem*. **2015**, *357*, 95–132.

(2) a) Rudolph, M.; Hashmi, A. S. K. Gold Catalysis in Total Synthesis - an Update. *Chem. Soc. Rev*. **2012**, *41*, 2448–2462; b) Pflästerer, D.; Hashmi, A. S. K. Gold Catalysis in Total Synthesis – Recent Achievements. *Chem. Soc. Rev*. **2016**, *45*, 1331-1367.

(3) a) Zi, W.; Toste, F. D. Recent Advances in Enantioselective Gold Catalysis *Chem. Soc. Rev*. **2016**, *45*, 4567-4589; b) Pradal, A.; Toullec, P. Y.; Michelet, V. Recent Developments in Asymmetric Catalysis in the Presence of Chiral Gold Complexes. *Synthesis* **2011**, 1501-1514; c) Sengupta, S.; Shi, X. Recent Advances in Asymmetric Gold Catalysis. *ChemCatChem* **2010**, *2*, 609-619; d) Widenhoefer, R. A. Recent Developments in Enantioselective Gold(I) Catalysis. *Chem. Eur. J*. **2008**, *14,* 5382-5391.

(4) a) Krause, N.; Winter, C. Gold-Catalyzed Nucleophilic Cyclization of Functionalized Allenes: A Powerful Access to Carbo- and Heterocycles. *Chem. Rev*. **2011**, *111*, 1994-2009; b) Shen, H. C. Recent Advances in Syntheses of Heterocycles and arbocycles via Homogeneous Gold Catalysis. Part 1: Heteroatom Addition and Hydroarylation Reactions of Alkynes, Allenes, and Alkenes. *Tetrahedron* **2008**, *64*, 3885-3903.

(5) a) Patil, N. T. Chirality Transfer and Memory of Chirality in Gold-Catalyzed Reactions. *Chem. Asian J*. **2012**, *7*, 2186 – 2194; b) Campolo, D.; Gastaldi, S.; Roussel, C.; Bertrand, M. P.; Nechab, M. Axial-to-Central Chirality Transfer in Cyclization Processes. *Chem. Soc. Rev*. **2013**, *42*, 8434--8466; c) Teller, H.; Corbet, M.; Mantilli, L.; Gopakumar, G.; Goddard, R.; Thiel W.; Fürstner, A. One-Point Binding Ligands for Asymmetric Gold Catalysis: Phosphoramidites with a TADDOL-Related but Acyclic Backbone. *J. Am. Chem. Soc*. **2012**, *134*, 15331-15342; d) Miles, D. H.; Veguillas, M.; Toste, F. D. Gold(I)-Catalyzed Enantioselective Bromocyclization Reactions of Allenes. *Chem. Sci*. **2013**, *4*, 3427-3431; e) Handa, S.; Lippincott, D. J.; Aue, D. H.; Lipshutz, B. H. Asymmetric Gold-Catalyzed

Lactonizations in Water at Room Temperature. *Angew. Chem., Int. Ed*. **2014**, *53*, 10658-10662; f) Zi, W.; Toste, F. D. Gold(I)-Catalyzed Enantioselective Desymmetrization of 1,3-Diols Through Intramolecular Hydroalkoxylation of Allenes. *Angew. Chem., Int. Ed.* **2015**, *54*, 14447-14451; g) Shu, X.-Z.; Nguyen, S. C.; He, Y.; Oba, F.; Zhang, Q.; Canlas, C.; Somorjai, G. A.; Alivisatos A. P.; Toste, F. D. Silica-Supported Cationic Gold(I) Complexes as Heterogeneous Catalysts for Regio- and Enantioselective Lactonization Reactions. *J. Am. Chem. Soc*. **2015**, *137*, 7083-7086.

(6) Cox, N.; Uehling, M. R.; Haelsig, K. T.; Lalic, G. Catalytic Asymmetric Synthesis of Cyclic Ethers Containing an α-Tetrasubstituted Stereocenter. *Angew. Chem. Int. Ed*. **2013**, *52*, 4878-4882.

(7) Wang, Z. J.; Benitez, D.; Tkatchouk, E.; Goddard, W. A.; Toste, F. D. Mechanistic Study of Gold(I)-Catalyzed Intermolecular Hydroamination of Allenes. *J. Am. Chem. Soc*. **2010**, *132*, 13064-13071.

(8) Liu, Z.; Wasmuth, A. S.; Nelson, S. G. Au(I)-Catalyzed Annulation of Enantioenriched Allenes in the Enantioselective Total Synthesis of (−)-Rhazinilam. *J. Am. Chem. Soc*. **2006**, *128*, 10352-10353.

(9) Zeldin, R. M.; Toste, F. D. Synthesis of Flinderoles B and C by a Gold-Catalyzed Allene Hydroarylation. *Chem. Sci*. **2011**, *2*, 1706-1709.

(10) Bates, R. W.; Dewey, M. R. A Formal Synthesis of Swainsonine by Gold-Catalyzed Allene Cyclization. *Org. Lett*. **2009**, *11*, 3706-3708.

(11) Sawama, Y.; Sawama, Y.; Krause, N. First Total Synthesis of (*R,R,R*)- and (3*R*,5*S*,9*R*)-Bejarol by Gold-Catalyzed Allene Cycloisomerization and Determination of Absolute Configuration of the Natural Product. *Org. Biomol. Chem.* **2008**, *6*, 3573-3579.

(12) Schmiedel, V. M.; Stefani, S.; Reissig, H.-U. Stereodivergent Synthesis of Jaspine B and its Isomers Using a Carbohydrate-Derived Alkoxyallene as C3-building Block. *Beilstein J. Org. Chem.* **2013**, *9*, 2564-2569.

(13) Jeker, O. F.; Carreira, E. M. Total Synthesis and Stereochemical Reassignment of (±)-Indoxamycin B. *Angew. Chem., Int. Ed*. **2012**, *51*, 3474-3477.

(14) Okada, T.; Sakaguchi, K.; Shinada, T.; Ohfune, Y. Total Synthesis of (−)-Funebrine via Au-Catalyzed Regio- and Stereoselective γ-Butyrolactonization of Allenylsilane. *Tedrahedron Lett*. **2011**, *52*, 5744-5746.

(15) Yang, W.; Hashmi, A. S. K. Mechanistic Insights into the Gold Chemistry of Allenes. *Chem. Soc. Rev*. **2014**, *43*, 2941-2955.

(16) a) Faza, O. N.; López, C. S. Computational Approaches to Homogeneous Gold Catalysis. *Top. Curr. Chem*. **2015**, 357, 213-283; b) Soriano E.; Fernández, I. Allenes and Computational Chemistry: From Bonding Situations to Reaction Mechanisms. *Chem. Soc. Rev*. **2014**, *43*, 3041-3105; c) Malacria, M.; Fensterbank, L.; Gandon, V. Activation of Allenes by Gold Complexes: A Theoretical Standpoint. *Top. Curr. Chem.* **2011**, *302*, 157-182; d) Alcaide, B.; Almendros, P.; Campo, T. M.; Soriano, E.; Marco-Contelles, J. Heterocyclization of Allenes Catalyzed by Late Transition Metals: Mechanisms and Regioselectivity. *Top. Curr. Chem*. **2011** *302*, 183-224; e) Montserrat, S.; Ujaque, G.; López, F.; Mascarenãs, J. L.; Lledós, A. Gold-Catalyzed Cycloadditions Involving Allenes: Mechanistic Insights from Theoretical Studies. *Top. Curr. Chem*. **2011**, *302*, 225-248; f) Gandon, V.; Lemiére, G.; Hours, A.; Fensterbank, L.; Malacria, M. The Role of Bent Acyclic Allene Gold Complexes in Axis-to-Center Chirality Transfers. *Angew. Chem. Int. Ed*. **2008**, *47*, 7534-7538; g) Montserrat, S.; Faustino, H.; Lledós, A.; Mascareñas, J. L.; López, F.; Ujaque, G. Mechanistic Intricacies of Gold-Catalyzed Intermolecular Cycloadditions between Allenamides and Dienes. *Chem. Eur. J.* **2013**, *19*, 15248-15260; h) Benitez, D.; Tkatchouk, E.; Gonzalez, A. Z.; Goddard, W. A.; Toste, F. D. On the Impact of Steric and Electronic Properties of Ligands on Gold(I)-Catalyzed Cycloaddition Reactions. *Org. Lett.* **2009**, *11*, 4798-4801; i) Zhu, R.-X.; Zhang, D.-J.; Guo, J.-X.; Mu, J.-L.; Duan, C.-G.; Liu, C.-B. Mechanism Study

of the Gold-Catalyzed Cycloisomerization of α-Aminoallenes: Oxidation State of Active Species and Influence of Counterion. *J. Phys. Chem. A* **2010**, *114*, 4689–4696.

(17) Paton, R. S.; Maseras, F. Gold(I)-Catalyzed Intermolecular Hydroalkoxylation of Allenes: A DFT Study. *Org. Lett.* **2009**, *11*, 2237-2240.

(18) For reviews on intermediates generated in gold(I) catalysis, including allene hydrofunctionalization see: a) Liu, L.-P.; Hammond, G. B. Recent Advances in the Isolation and Reactivity of Organogold Complexes. *Chem. Soc. Rev*. **2012**, *41*, 3129-3139; b) Obradors, C.; Echavarren, A. M. Intriguing Mechanistic Labyrinths in Gold(I) Catalysis. *Chem. Commun*. **2014**, *50*, 16-28; c) Lauterbach, T. Asirib, A. M. Hashmi, A. S. K. Chapter Five - Organometallic Intermediates of Gold Catalysis. *Adv. Organomet. Chem*. **2014**, *62*, 261-297; d) Ranieri, B.; Escofeta, I.; Echavarren, A. M.; Anatomy of Gold Catalysts: Facts and Myths. *Org. Biomol. Chem*. **2015**, *13*, 7103-7118; e) Jones, A. C. Gold π-Complexes as Model Intermediates in Gold Catalysis. *Top. Curr. Chem*. **2015**, *357*, 133-165; f) Weber, D.; Gagne, M. R. Aurophilicity in Gold(I) Catalysis: for Better or Worse? *Top. Curr. Chem*. **2015**, *357*, 167-211; g) Brooner, R. E. M.; Widenhoefer, R. A. Cationic, Two-Coordinate Gold π-Complexes. *Angew. Chem. Int. Ed*. **2013**, *52*, 11714-11724; h) Schmidbaur, H.; Schier, A. Gold η^2-Coordination to Unsaturated and Aromatic Hydrocarbons: The Key Step in Gold-Catalyzed Organic Transformations. *Organometallics* **2010**, *29*, 2-23.

(19) a) Brown, T. J.; Sugie, A.; Dickens, M. G.; Widenhoefer, R. A. Structures and Dynamic Solution Behavior of Cationic, Two-Coordinate Gold(I)–π-Allene Complexes. *Chem. Eur. J*. **2012**, *18*, 6959-6971; b) Brown, T. J.; Sugie, A.; Dickens, M. G.; Widenhoefer, R. A. Solid-State and Dynamic Solution Behavior of a Cationic, Two-Coordinate Gold(I) π-Allene Complex. *Organometallics* **2010**, *29*, 4207-4209.

(20) Brooner, R. E. M.; Brown, T. J.; Widenhoefer, R. A. Synthesis and Study of Cationic, Two-Coordinate Triphenylphosphine–Gold– π-Complexes. *Chem. Eur. J*. **2013**, *19*, 8276-8284.

(21) a) Liu, L.-P.; Xu, B.; Mashuta, M. S.; Hammond, G. B. Synthesis and Structural Characterization of Stable Organogold(I) Compounds. Evidence for the Mechanism of Gold-Catalyzed Cyclizations. *J. Am. Chem. Soc*. **2008**, *130*, 17642-17643; b) Liu, L.-P.; Hammond, G. B. Reactions of Cationic Gold(I) with Allenoates: Synthesis of Stable Organogold(I) Complexes and Mechanistic Investigations on Gold-Catalyzed Cyclizations. *Chem.–Asian J*. **2009**, *4*, 1230-1236; c) Shi, Y.; Roth, K. E.; Ramgren, S. D.; Blum, S. A. Catalyzed Catalysis Using Carbophilic Lewis Acidic Gold and Lewis Basic Palladium: Synthesis of Substituted Butenolides and Isocoumarins. *J. Am. Chem. Soc*. **2009**, *131*, 18022-18023.

(22) a) Weber, D.; Tarselli, M. A.; Gagné, M. R. Mechanistic Surprises in the Gold(I)-Catalyzed Intramolecular Hydroarylation of Allenes. *Angew. Chem., Int. Ed*. **2009**, *48*, 5733-5736; b) Weber, D.; Gagné, M. R. Dinuclear Gold−Silver Resting States May Explain Silver Effects in Gold(I)-Catalysis. *Org. Lett*. **2009**, *11*, 4962-4965; c) Weber, D.; Gagné, M. R. σ–π-Diauration as an Alternative Binding Mode for Digold Intermediates in Gold(I) Catalysis. *Chem. Sci*. **2013**, *4*, 335-338.

(23) Brown, T. J.; Weber, D.; Gagné, M. R.; Widenhoefer, R. A. Mechanistic Analysis of Gold(I)-Catalyzed Intramolecular Allene Hydroalkoxylation Reveals an Off-Cycle Bis(gold) Vinyl Species and Reversible C–O Bond Formation. *J. Am. Chem. Soc*. **2012**, *134*, 9134-9137.

(24) For additional examples of gold vinyl complexes generated via nucleophilic addition to alkynes or transmetallation see: a) Akana, J. A.; Bhattacharyya, K. X.; Müller, P.; Sadighi, J. P. Reversible C−F Bond Formation and the Au-Catalyzed Hydrofluorination of Alkynes. *J. Am. Chem. Soc*. **2007**, *129*, 7736-7737; b) Hashmi, A. S. K.; Wieteck, M.; Braun, I.; Nösel, P.; Jongbloed, L.; Rudolph, M.; Rominger, F. Gold-Catalyzed Synthesis of Dibenzopentalenes – Evidence for Gold Vinylidenes. *Adv.*

Synth. Catal. **2012**, *354*, 555-562. c) Hashmi, A. S. K.; Schuster, A. M.; Rominger, F. Mechanism of the Transmetalation of Organosilanes to Gold. *Angew. Chem., Int. Ed*. **2009**, *48*, 8247-8249; d) Hashmi, A. S. K.; Schuster, A. M.; Gaillard, S.; Cavallo, L.; Poater, A.; Nolan, S. P. Selectivity Switch in the Synthesis of Vinylgold(I) Intermediates. *Organometallics* **2011**, *30*, 6328-6337; e) Hashmi, A. S. K.; Ramamurthi, T. D.; Rominger, F. On the Trapping of Vinylgold Intermediates. *Adv. Synth. Catal.* **2010**, *352*, 971-975; f) Zeng, X.; Kinjo, R.; Donnadieu, B.; Bertrand, G. Serendipitous Discovery of the Catalytic Hydroammoniumation and Methylamination of Alkynes. *Angew. Chem., Int. Ed*. **2010**, *49*, 942-945; g) Chen, Y.; Wang, D.; Petersen, J. L.; Akhmedov, N. G.; Shi, X. Synthesis and Characterization of Organogold Complexes Containing an Acid Stable Au–C Bond Through Triazole-yne 5-*endo*-dig Cyclization. *Chem. Commun*. **2010**, *46*, 6147-6149; h) Seidel, G.; Lehmann, C. W.; Fürstner, A. Elementary Steps in Gold Catalysis: The Significance of *gem*-Diauration. *Angew. Chem. Int*. Ed. **2010**, *49*, 8466-8470; i) Hashmi, A. S. K.; Braun, I.; Nösel, P.; Schädlich, J.; Wieteck, M.; Rudolph, M.; Rominger, F. Simple Gold-Catalyzed Synthesis of Benzofulvenes—gem-Diaurated Species as "Instant Dual-Activation" Precatalysts. *Angew. Chem. Int. Ed.* **2012**, *51*, 4456-4460; j) Hashmi, A. S. K.; Braun, I.; Rudolph, M.; Rominger, F. The Role of Gold Acetylides as a Selectivity Trigger and the Importance of *gem*-Diaurated Species in the Gold-Catalyzed Hydroarylating-Aromatization of Arene-Diynes. *Organometallics* **2012**, *31*, 644-661.

(25) Zhang, Z.; Widenhoefer, R. A. Regio- and Stereoselective Synthesis of Alkyl Allylic Ethers via Gold(I)-Catalyzed Intermolecular Hydroalkoxylation of Allenes with Alcohols. *Org. Lett*. **2008**, *10*, 2079-2081.

(26) Zhang, Z.; Liu, C.; Kinder, R. E.; Han, X.; Qian, H.; Widenhoefer, R. A. Highly Active Au(I) Catalyst for the Intramolecular *exo*-Hydrofunctionalization of Allenes with Carbon, Nitrogen, and Oxygen Nucleophiles. *J. Am. Chem. Soc*. **2006**, *128*, 9066-9073.

(27) a) Gockel, B.; Krause, N. Golden Times for Allenes: Gold-Catalyzed Cycloisomerization of β-Hydroxyallenes to Dihydropyrans. *Org. Lett*. **2006**, *8*, 4485-4488; b) Zhang, Z.; Widenhoefer, R. A. Gold(I)-Catalyzed Intramolecular Enantioselective Hydroalkoxylation of Allenes. *Angew. Chem., Int. Ed.* **2007**, *46*, 283-285; c) Winter, C.; Krause, N. Structural Diversity through Gold Catalysis: Stereoselective Synthesis of *N*-Hydroxypyrrolines, Dihydroisoxazoles, and Dihydro-1,2-oxazines. *Angew. Chem., Int. Ed*. **2009**, 48, 6339-6342; d) Morita, N.; Krause, N. The First Gold-Catalyzed C-S Bond Formation: Cycloisomerization of α-Thioallenes to 2,5-Dihydrothiophenes. *Angew. Chem., Int. Ed.* **2006**, 45, 1897-1899; e) Zhang, Z.; Bender, C. F.; Widenhoefer, R. A. Gold(I)-Catalyzed Dynamic Kinetic Enantioselective Intramolecular Hydroamination of Allenes. *J. Am. Chem. Soc.* **2007**, *129*, 14148-14149.

(28) Similar conclusions were drawn by Maier and Zhdanko regarding the gold(I)-catalyzed intramolecular hydroalkoxylation of alkynes: a) Zhdanko, A.; Maier, M. E. Synthesis of *gem*-Diaurated Species from Alkynols. *Chem. Eur. J*. **2013**, *19*, 3932-3942; b) Zhdanko, A.; Maier, M. E. Quantitative Evaluation of the Stability of *gem*-Diaurated Species in Reactions with Nucleophiles. *Organometallics* **2013**, *32*, 2000-2006; c) Zhdanko, A.; Maier, M. E. The Mechanism of Gold(I)-Catalyzed Hydroalkoxylation of Alkynes: An Extensive Experimental Study. *Chem. Eur. J*. **2014**, *20*, 1918-1930.

(29) a) Zhdanko, A.; Maier, M, E. Explanation of "Silver Effects" in Gold(I)-Catalyzed Hydroalkoxylation of Alkynes. *ACS Catal.* **2015**, *5*, 5994−6004; b) Wang, D.; Cai, R.; Sharma, S.; Jirak, J.; Thummanapelli, S. K.; Akhmedov, N. G.; Zhang, H.; Liu, X.; Petersen, J. L.; Shi, X. "Silver Effect" in Gold(I) Catalysis: An Overlooked Important Factor. *J. Am. Chem. Soc*. **2012**, *134*, 9012−9019; c) Homs, A.; Escofet, I.; Echavarren, A. M. On the Silver Effect and the Formation of Chloride-Bridged Digold Complexes. *Org. Lett.* **2013**, *15*, 5782−5785; d) Kumar, M.; Hammond, G. B.; Xu, B. Cationic Gold Catalyst Poisoning and Reactivation. *Org. Lett.* **2014**, *16*, 3452−3455; e) Zhu, Y.; Day, C. S.;

Zhang, L.; Hauser, K. J.; Jones, A. C. A Unique Au–Ag–Au Triangular Motif in a Trimetallic Halonium Dication: Silver Incorporation in a Gold(I) Catalyst. *Chem. Eur. J.* **2013**, *19*, 12264 – 12271.

(30) Brown, T. J.; Dickens, M. G.; Widenhoefer, R. A. Syntheses, X-ray Crystal Structures, and Solution Behavior of Monomeric, Cationic, Two-Coordinate Gold(I) π-Alkene Complexes. *J. Am. Chem. Soc*. **2009**, *131*, 6350-6351.

(31) Cornell, T. P.; Shi, Y.; Blum, S. A. Synthesis of Alkenylgold(I) Compounds via Sequential Hydrozirconation and Zirconium to Gold Transmetalation. *Organometallics* **2012**, *31*, 5990−5993.

(32) Hashmi, A. S. K. Dual Gold Catalysis. *Acc. Chem. Res.* **2014**, *47,* 864–876.

(33) As a caveat, the ^{13}C NMR resonance of the carbene C1 resonance of **6** could not be determined in toluene-d_8 and the carbene C1 resonance of **6** obtained in CD_2Cl_2 (δ 161) differs from that of (IPr*)AuOTf (δ 163) by only ~2 ppm, which offers the possibility of accidental equivalence of the ^{13}C NMR resonances of (IPr*)AuOTf and **6** in toluene-d_8. However, Zhdanko and Maier have shown that the binding affinity of methanol to the (L)Au$^+$ fragment in $CDCl_3$ is several orders of magnitude lower than that of C–C multiple bonds, consistent with the absence of detectable binding of **2** to (IPr)Au$^+$ in toluene-d_8.[34]

(34) Zhdanko, A.; Ströbele, M.; Maier, M. E. Coordination Chemistry of Gold Catalysts in Solution: A Detailed NMR Study. *Chem. Eur. J.* **2012**, *18*, 14732 – 14744.

(35) a) Mukherjee, P.; Widenhoefer, R. A. The Regio- and Stereospecific Intermolecular Dehydrative Alkoxylation of Allylic Alcohols Catalyzed by a Gold(I) *N*-Heterocyclic Carbene Complex. *Chem. Eur. J*. **2013**, *19*, 3437–3444; b) Aponick, A.; Biannic, B. Gold-Catalyzed Dehydrative Cyclization of Allylic Diols. *Synthesis* **2008**, 3356-3359; c) Aponick, A.; Li, C.-Y.; Palmes, J. A. Au-Catalyzed Cyclization of Monopropargylic Triols: An Expedient Synthesis of Monounsaturated Spiroketals. *Org. Lett*. **2009**, *11*, 121-124; d) Aponick, A.; Li, C.-Y.; Biannic, B. Au-Catalyzed Cyclization of Monoallylic Diols. *Org. Lett.*

2008, *10*, 669-671; e) Aponick, A.; Biannic, B.; Jong, M. R. A Highly Adaptable Catalyst/Substrate System for the Synthesis of Substituted Chromenes. *Chem. Commun*. **2010**, *46*, 6849-6851; f) Bandini, M.; Monari, M.; Romaniello, A.; Tragni, M. Gold-Catalyzed Direct Activation of Allylic Alcohols in the Stereoselective Synthesis of Functionalized 2-Vinyl-Morpholines. *Chem. Eur. J.* **2010**, *16*, 14272-14277; g) Biannic, B.; Aponick, A. A Comparative Study of the Au-Catalyzed Cyclization of Hydroxy-Substituted Allylic Alcohols and Ethers. *Bielstein J. Org. Chem.* **2011**, *7*, 802-807; h) Aponick, A.; Biannic, B. Chirality Transfer in Au-Catalyzed Cyclization Reactions of Monoallylic Diols: Selective Access to Specific Enantiomers Based on Olefin Geometry. *Org. Lett*. **2011**, *13*, 1330-1333; i) Ghebreghiorgis, T.; Biannic, B.; Kirk, B. H.; Ess, D. H.; Aponick, A. The Importance of Hydrogen Bonding to Stereoselectivity and Catalyst Turnover in Gold-Catalyzed Cyclization of Monoallylic Diols. *J. Am. Chem. Soc*. **2012**, *134*, 16307-16318; j) Barker, G.; Johnson, D. G.; Young, P. C.; Macgregor, S. A.; Lee, A.-L. Chirality Transfer in Gold(I)-Catalysed Direct Allylic Etherifications of Unactivated Alcohols: Experimental and Computational Study. *Chem. Eur. J.* **2015**, 21, 13748 – 13757; k) Coutant, E.; Young, P. C.; Barker, G.; Lee, A.-L. Gold(I)-Catalysed One-Pot Synthesis of Chromans Using Allylic Alcohols and Phenols. *Beilstein J. Org. Chem*. **2013**, *9*, 1797–1806.

(36) Hadfield, M. S.; Lee, A.-L. Regioselective Synthesis of *tert*-Allylic Ethers via Gold(I)-Catalyzed Intermolecular Hydroalkoxylation of Allenes. *Org. Lett.* **2010**, *12*, 484-487.

(37) The protodeauration of gold vinyl complexes with retention of configuration has been established experimentally: Hashmi, A. S. K.; Ramamurthi, T. D.; Rominger, F. Synthesis, Structure and Reactivity of Organogold Compounds of Relevance to Homogeneous Gold Catalysis. *J. Organomet. Chem*. **2009**, *694*, 592–597.

(38) Briggs, G. E.; Haldane, J. B. S. A Note on the Kinetics of Enzyme Action. *Biochem. J.* **1925**, *19*, 338–339.

(39) a) Kochi, J. K.; Bockman, T. M. Organometallic Ions and Ion Pairs. *Adv. Organomet. Chem*. **1991**, *33*, 51-124; b) Macchioni, A. Ion Pairing in Transition-Metal Organometallic Chemistry. *Chem. Rev*. **2005**, *105*, 2039-2073.

(40) a) Zuccaccia, D.; Belpassi, L.; Macchioni, A.; Tarantelli, F. Ligand Effects on Bonding and Ion Pairing in Cationic Gold(I) Catalysts Bearing Unsaturated Hydrocarbons. *Eur. J. Inorg. Chem*. **2013**, 4121–4135; b) Zuccaccia, D.; Belpassi, L.; Rocchigiani, L.; Tarantelli, F.; Macchioni, A. A Phosphine Gold(I) π-Alkyne Complex: Tuning the Metal−Alkyne Bond Character and Counterion Position by the Choice of the Ancillary Ligand. *Inorg. Chem.* **2010**, *49*, 3080–3082; c) Zuccaccia, D.; Belpassi, L.; Tarantelli, F.; Macchioni, A. Ion Pairing in Cationic Olefin−Gold(I) Complexes. *J. Am. Chem. Soc*. **2009**, *131*, 3170–3171.

(41) Song, L.; Trogler, W. C. Mechanism of Halide-Induced Disproportionation of $M(CO)_3(PCy_3)^{2+}$ 17-Electron Radicals (M = Fe, Ru, Os). Periodic Trends on Reactivity and the Role of Ion Pairs. *J. Am. Chem. Soc.* **1992**, *114*, 3355-3361.

(42) Alibrandi, C.; Romeo, R.; Scolaro, L. M.; Tobe, M. L. The Ion-Pair Mechanism in Square Planar Substitution. Displacement of Dimethyl Sulfoxide from Chloro(dimethylsulfoxide)(*N,N,N'N'*-tetramethyldiaminoethane)platinum(II) Salts by Halide Ions in Dichloromethane Solution. *Inorg. Chem*. **1992**, *31*, 5061-5066.

(43) Marcus, Y.; Hefter, G. Ion Pairing. *Chem. Rev.* **2006**, *106*, 4585-4621.

(44) Worth noting is that even under conditions of excess **2**, the reaction medium for hydroalkoxylation is relatively non-polar. For example, the dielectric constant for a binary solvent mixture can be calculated from the relationship $\varepsilon_m = \chi_1\varepsilon_1 + \chi_2\varepsilon_2$, where χ_1 and χ_2 are the mole fractions of solvent 1 and 2, respectively.[45] Using this relationship and using the dielectric constant of phenethylalcohol (ε = 8.9) as a reasonable approximation for the dielectric constant of **2**,[46] a 2.7 M solution of **2** in toluene has a calculated dielectric constant of ε_m = 0□□□□×□□□□ + 0.68 × □□□□ = 4.5.

(45) Jouyban, A.; Soltanpour, S. Prediction of Dielectric Constants of Binary Solvents at Various Temperatures. *J. Chem. Eng. Data* **2010**, *55*, 2951–2963.

(46) Maryott, A. A.; Smith, E. R. *Table of dielectric constants of pure liquids*, Circular of the National Bureau of Standards, 514; Washington, D.C.; U. S. Gov. Print. Office, 1951.

(47) a) Romeo, R.; Arena, G.; Scolaro, L. M.; Plutino, M. R. Ion-Pair Mechanism in Square Planar Substitution. Reactivity of Cationic Platinum (II) Complexes with Negatively Charged Nucleophiles in Solvents of High, Medium and Low Polarity. *Inorg. Chim. Acta* **1995**, *240*, 81-92; b) Romeo, R.; Nastasi, N.; Scolaro, L. M.; Plutino, M. R.; Albinati, A.; Macchioni, A. Molecular Structure, Acidic Properties, and Kinetic Behavior of the Cationic Complex (Methyl)(dimethylsulfoxide)(bis-2-pyridylamine)platinum(II) Ion. *Inorg. Chem*. **1998**, *37*, 5460-5466; c) Aizawa, S.-i.; Sone, Y.; Kawamoto, T.; Yamada, S.; Nakamura, M. Kinetic Studies on Thiolato-Ligand Substitution Reactions with Halide Ions of Square-Planar Palladium(II) Complex with Bis(2-(diphenylphosphino)ethyl)phenylphosphine. *Inorg. Chim. Acta* **2002**, *338*, 235-239.

(48) This rate equation assumes a mechanism for ligand exchange involving interchange through a tight ion pair. The $k_{-1}K_A$[OTf] term in the denominator of eq 11 becomes k_{-1}[OTf] if ligand exchange occurs without ion pair association through an associative pathway. These pathways are kinetically indistinguishable in the absence of ion pairing.

(49) This rate law was derived assuming that **2** reacts with both **5** and **5**•OTf and with identical microscopic rate constants k_2. We likewise derived a pair of limiting rate equations assuming that C–O bond formation occurred exclusively via attack of **2** on either the ion-paired (**5**•OTf) or ionized (**5**) form of the π-allene complex (see Supporting Information). While the former rate equation was fully consistent with our experimental data, the latter predicted inhibition by triflate even under conditions of strong ion pairing and was therefore inconsistent with our experimental observations.

(50) a) Rocchigiani, L.; Bellachioma, G.; Ciancaleoni, G.; Crocchianti, S.; Laganà, A.; Zuccaccia, C.; Zuccaccia, D.; Macchioni A. Anion-Dependent Tendency of Di-Long-Chain Quaternary Ammonium Salts to Form Ion Quadruples and Higher Aggregates in Benzene. *ChemPhysChem* **2010**, *11*, 3243 – 3254; b) Mo, H.; Wang, A.; Wilkinson, P. S.; Pochapsky, T. C. Closed-Shell Ion Pairs: Cation and Aggregate Dynamics of Tetraalkylammonium Salts in an Ion-Pairing Solvent. *J. Am. Chem. Soc.* **1997**, *119*, 11666-11673.

(51) This analysis is complicated even further because the [(*n*-Bu_4)N][OTf] ion pairs likely associate further to form ion quadruples and higher aggregates.[50]

(52) Kinder, R. E.; Zhang, Z.; Widenhoefer, R. A. Intermolecular Hydroamination of Allenes with *N*-Unsubstituted Carbamates Catalyzed by a Gold(I) *N*-Heterocyclic Carbene Complex. *Org. Lett*. **2008**, *10*, 3157-3159.

(53) a) Roth K. E.; Blum, S. A. Relative Kinetic Basicities of Organogold Compounds. *Organometallics* **2010**, *29*, 1712-1716; b) Gaggioli, C. A.; Ciancaleoni, G.; Zuccaccia, D.; Bistoni, G.; Belpassi, L.; Tarantelli, F.; Belanzoni, P. Strong Electron-Donating Ligands Accelerate the Protodeauration Step in Gold(I)-Catalyzed Reactions: A Quantitative Understanding of the Ligand Effect. *Organometallics* **2016**, *35*, 2275−2285; c) Ahmadi, R. B.; Ghanbari, P.; Rajabi, N. A.; Hashmi, A. S. K.; Yates, B. F.; Ariafard, A. A Theoretical Study on the Protodeauration Step of the Gold(I)-Catalyzed Organic Reactions. *Organometallics* **2015**, *34*, 3186−3195.

(54) A gold η^1-allylic cation has been directly observed: Tudela, E.; González, J.; Vicente, R.; Santamaría, J.; Rodríguez, M. A.; Ballesteros, A. Mechanistic Studies on the Rearrangement of 1-Alkenyl-2-alkynylcyclopropanes: From Allylic Gold(I) Cations to Stable Carbocations. *Angew. Chem. Int. Ed*. **2014**, *53*, 12097 –12100.

(55) For the kinetic analysis of the gold(I)-catalyzed racemization of axially chiral allenes see: a) Li,

H.; Harris, R. J.; Nakafuku, K.; Widenhoefer, R. A. Kinetics and Mechanism of Allene Racemization Catalyzed by a Gold N-Heterocyclic Carbene Complex. *Organometallics* **2016**, *35*, 2242−2248; b) Harris, R.; Nokafuku, N.; Li, H.; Widenhoefer, R. A. Kinetics and Mechanism of the Racemization of Aryl Allenes Catalyzed by Cationic Gold(I) Phosphine Complexes. *Chem. Eur. J.* **2014**, *20*, 12245-12254.

(56) a) Eisenstein, O.; Hoffmann, R. Transition-Metal Complexed Olefins: How Their Reactivity Toward a Nucleophile Relates to Their Electronic Structure. *J. Am. Chem. Soc*. **1981**, *103*, 4308-4320; b) Cameron, A. D.; Smith, V. H.; Baird, M. C. A Reconsideration of the Role of Slippage in the Activation of Co-ordinated Olefins Towards Nucleophilic Attack. *J. Chem. Soc., Dalton Trans*. **1988**, 1037-1043.

(57) a) Zhdanko, A.; Maier, M. E. Explanation of Counterion Effects in Gold(I)-Catalyzed Hydroalkoxylation of Alkynes. *ACS Catal.* **2014**, 4, 2770−2775; b) Ciancaleoni, G.; Belpassi, L.; Zuccaccia, D.; Tarantelli, F.; Belanzoni, P. Counterion Effect in the Reaction Mechanism of NHC Gold(I)-Catalyzed Alkoxylation of Alkynes: Computational Insight into Experiment. *ACS Catal*. **2015**, *5*, 803−814; c) Biasiolo, L.; Trinchillo, M.; Belanzoni, P.; Belpassi, L.; Busico, V.; Ciancaleoni, G.; D'Amora, A.; Macchioni, A.; Tarantelli, F.; Zuccaccia, D. Unexpected Anion Effect in the Alkoxylation of Alkynes Catalyzed by *N*-Heterocyclic Carbene (NHC) Cationic Gold Complexes. *Chem. Eur. J.* **2014**, *20*, 14594 – 14598.

(58) Brown, T. J.; Brooner, R. E. M.; Chee, M. A.; Widenhoefer, R. A. Effect of Substitution, Ring Size, and Counterion on the Intermediates Generated in the Gold-Catalyzed Intramolecular Hydroalkoxylation of Allenes. *Organometallics* **2016**, *35*, 2014−2021.

TOC graphic

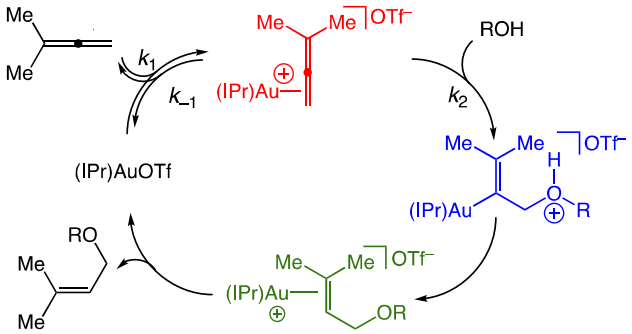
Me
Me
k_1
k_{-1}
(IPr)AuOTf
Me
Me
OTf⁻
(IPr)Au
ROH
k_2
Me
Me
OTf⁻
H
O
R
(IPr)Au
Me
Me
OTf⁻
(IPr)Au
OR
RO
Me
Me